Single-Molecule Trapping Dynamics of Sugar-Uptake Channels in Marine Bacteria

Wipa Suginta

Biochemistry-Electrochemistry Research Unit, Schools of Chemistry and Biochemistry, Institute of Science, Suranaree University of Technology, Nakhon Ratchasima 30000, Thailand

M. F. Smith*

School of Physics, Institute of Science, Suranaree University of Technology, Nakhon Ratchasima 30000, Thailand and Thailand Center of Excellence in Physics (ThEP), Commission of Higher Education, Ministry of Education, Bangkok 10400, Thailand

(Received 25 March 2013; published 4 June 2013)

Stochastic fluctuations of ion current through one chitoporin (ChiP) channel within a bilayer lipid membrane in sugar solution are analyzed. These reflect single-molecule dynamics, which indicate that ChiP has multiple binding sites for sugar and exploits interactions between bound molecules to direct sugar passage. Since ChiP is used by marine bacteria, this is likely an adaptive strategy to enhance sugar translocation from rough water.

DOI: 10.1103/PhysRevLett.110.238102 PACS numbers: 87.16.dp, 87.14.ep, 87.15.hj, 87.15.Vv

Some gram-negative bacteria uptake sugar from ambient fluid through a protein channel, which is an assembly of nanotubes, in their cell membrane [1]. Molecules of a specific sugar that diffuse into the channel can become trapped, remaining bound in a nanotube for many milliseconds before escaping into the cell. A bound molecule obstructs a nanotube so measurements of ionic current through a channel in sugar solution exhibit stepwise changes that track single-molecule dynamics on the millisecond time scale [2–4]. By studying the current profile of channels used by different bacteria, adaptive channel designs can be studied quantitatively.

The bioluminescent bacterium *V. harveyi* is responsible for the disease luminous Vibriosis, a leading cause of death in fish and prawn farms [5,6]. Having a high growth rate and able to survive extreme conditions, the bacteria effect rapid turnover of chitin in marine ecosystems. The bacterium degrades chitin into smaller sugar molecules and selectively uptakes chitohexaose through a channel called chitoporin (or ChiP) [7–14]. ChiP is a trimer, composed of three identical nanotubes (monomers) and thus, similar to other channels, like maltoporin from *E. coli* [1,15–18]. But ChiP operates in more demanding rough-water conditions and, accordingly, translocates sugar across a lipid bilayer more rapidly by orders of magnitude [19] than comparable channels [20–23].

In this Letter, we present data of ion current fluctuations $I(t)$ through a bilayer lipid membrane immersed in chitohexaose solution and perforated with one trimeric ChiP. $I(t)$ fluctuates among discrete bands such that $I(t) \approx I_n = I_0(3 - n)/3$ when n monomers are blocked by sugar. By analyzing the stochastic integer n, we find that (i) each ChiP monomer functions independently, (ii) a monomer has multiple binding sites (or traps) that can be occupied simultaneously, and (iii) there is evidence that molecules bound in the same monomer attract each other.

The results indicate a multiple-trap design that could explain how ChiP uptakes sugar so effectively. Studies on maltoporin were interpreted using single trap models [24]. While one trap is sufficient for uptaking sugar from a congenial environment, multiple traps can stream sugar across the membrane more rapidly. Using the intuitive population-decay approach developed below, multiple-molecule trapping by ChiP is evident from data. This offers advantages over power-spectral analysis, widely used to interpret similar $I(t)$ data, in which such essential properties are identified using fits to model calculations.

We now present details [25]. Two chambers, separated by a 25 μm thick Teflon film barrier with a 30 μm radius aperture, are filled with 1M of KCl. Ag/AgCl electrodes are immersed on respective sides of the barrier. After adding the lipid DPhPC, a bilayer is formed over the aperture [26]. A 100 mV bias produces no current, so the bilayer is impenetrable to K^+ and Cl^- ions. A few minutes after 50–100 ng/mL of *Vh*ChiP is added to the cis side of the membrane, a step increase of $I(t)$ is seen, indicating that the first channel has opened in the bilayer. Here, the cis side of the membrane is defined as the side at higher electrical potential than the opposite, trans side. Studies of maltoporin indicate that the natural mouth of the channel points towards the chamber to which the precursor (*Vh*ChiP) is added, so we regard the cis side as being analogous to the cell exterior [27,28]. After the first ChiP insertion, the protein solution was gently diluted by sequential additions of electrolyte to prevent further insertions.

The current through the open trimer averaged $I_0 \approx$ 186 pA with a 100 mV bias. $I(t) - I_0$ can be fit by a Gaussian with standard deviation $\sigma_0 \approx 8$ pA. With chitohexaose added to the cis side, $I(t)$ fluctuated between bands I_n, see Fig. 1. Band transitions in Fig. 1 indicate that a molecule can enter or leave a monomer in roughly $t_{\min} =$ 0.1 ms. When a molecule enters an unoccupied monomer,

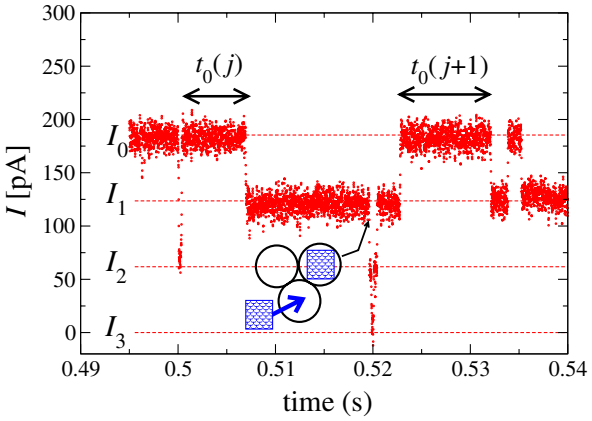

FIG. 1 (color online). Dynamical trapping of single sugar molecules by a ChiP protein channel. The ion current $I(t)$ measured through a single ChiP, which perforates an otherwise intact lipid bilayer, with a sugar concentration of 5 μM on one side of the membrane is measured versus time. The ChiP consists of three identical tubes (or monomers) and the ion current fluctuates such that $I(t) \approx I_n = I_0(3-n)/n$ with $n = 0$, 1, 2, 3 when n monomers are blocked by sugar molecules. $I(t)$ remains in a band for a time $t_n[j]$, where j counts each occurrence, then makes a transition associated with either trapping or detrapping of a single molecule. An $I_1 \rightarrow I_2$ trapping event is illustrated by the cartoon: with one monomer already blocked, a second monomer traps a sugar molecule, resulting in a current decrease.

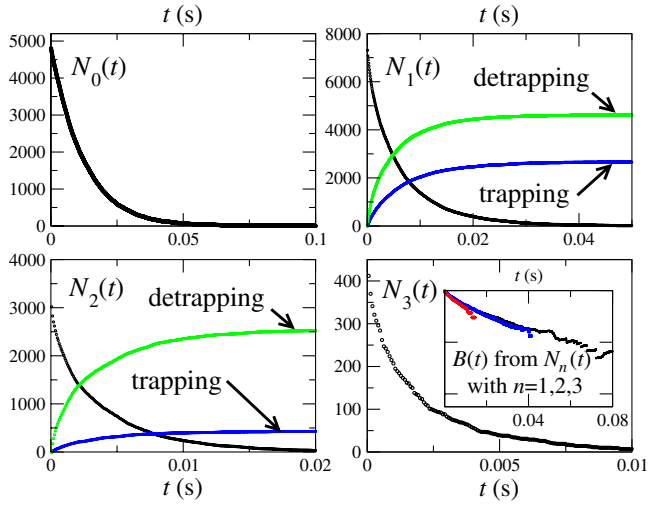

FIG. 2 (color online). Plots of $N_n(t)/N_n(0)$, which is the probability that n monomers of the ChiP trimer remain continuously blocked by sugar molecules bound within them for longer than t. $N_n(t)$ is obtained from $I(t)$ data, like that in Fig. 1, by counting the number of different j for which $t_n[j] > t$. For $n = 0$ ($n = 3$) all segments end when an open (blocked) monomer becomes blocked (open), which we call trapping (detrapping). For $n = 1$, 2, both processes occur. The inset in the lower right shows the $B(t)$ (the logarithm of the probability for a single monomer to remain blocked for time t) as determined from the $n = 1$, 2, and 3 distributions. The fact that they agree means that different monomers in the trimer act independently.

n increases by one. The fact that n can then remain constant for a time $t_n[j] \gg t_{\min}$ means that molecules can be chemically bound (i.e., "trapped") in a monomer [29]. Thermal fluctuations provide the rare, sudden events in which a molecule escapes (i.e., "detraps"). If the escape empties the monomer then n decreases by one.

We record times $t_n[j]$, over which the current remains continuously in band n, where j counts each occurrence. Small values $t_n[j] < t_{\min} = 0.1$ ms are ignored (if $I(t)$ fluctuates away from n but returns within $t_{\min}$ then it is treated as if it never left n). Fluctuations on a time scale less than $t_{\min}$, which could result from a molecule diffusing into a monomer without becoming bound (as well as outlying points of Gaussians straying between bands), are not studied. Correlations between $t_n[j]$ (for the same n but different j) are assessed using the function, $\chi_n(s) \equiv \sum_j (t_n[j] - \bar{t}_n)(t_n[j+s] - \bar{t}_n)/\bar{t}_n^2$ where s is an integer and $\bar{t}_n$ is the average of $t_n[j]$ over all j.

The measured quantity $N_n(t)$ is the number of j for which $t_n[j] > t$. $N_n(t)/N_n(0)$ is interpreted as the probability for n monomers to remain continuously blocked for a time longer than t. Sample distributions $N_n(t)$ are shown in Fig. 2. Almost all $t_n[j]$ ended with a transition in which n changes by $\Delta n = \pm 1$. Events with $|\Delta n| > 1$ were too rare to treat statistically. For an open trimer, $\chi_0(1)/\chi_0(0) \approx 0.01$ for a sample size $N_0(0) \approx 4800$. While for a trimer with one blocked monomer, the value $\chi_1(1)/\chi_1(0) \approx 0.06$ for $N_1(0) \approx 7500$. These weak correlations indicate that $t_n[j]$ and $t_n[j' \neq j]$ are approximately independent.

To determine if trapping in different monomers is correlated, we compare $N_n(t)$ for the trimer to that expected for three independent monomers. We define the probability for a monomer, initially unblocked, to remain continuously unblocked for more than t as $\exp(U[t])$ and the probability for a monomer, initially blocked, to remain continuously blocked for more than t as $\exp(B[t])$. For identical, independent monomers

$$\ln N_n(t) - \ln N_n(0) = (3-n)U(t) + nB(t). \quad (1)$$

Equation (1) relates four measured $N_n(t)$ to two unknowns $U(t)$ and $B(t)$, and can be checked for consistency. Using Eq. (1), we obtained $U(t)$ from $N_0(t)$ and then used $n = 1$, 2, 3 to obtain three estimates of $B(t)$. These estimates, shown together in Fig. 2, agree. This rules out significant correlation between monomers. Each monomer acts independently.

Henceforth, we study a single monomer, characterized by $U(t)$ and $B(t)$. $U(t)$ describes trapping by an open monomer and $B(t)$ describes detrapping from an occupied monomer. Note that the $I(t)$ measurement cannot determine how many molecules occupy a monomer (the first molecule blocks the current so the arrival or departure of

additional molecules has no effect). If a monomer becomes occupied at $t = 0$ then $\exp[B(t)]$ is the probability for it to remain occupied, by at least one molecule, beyond time t.

In Fig. 3, $U(t)$ and $B(t)$ are shown for a range of sugar concentrations $[c]$ on the cis side. $U(t)$ is approximately

$$U(t) \approx -k_{\text{on}}[c]t, \tag{2}$$

where the empirical parameter $k_{\text{on}}[c]$ can be understood as the rate at which sugar molecules are trapped by an open monomer. With a factor of $[c]$ removed, k_{on} is the trapping rate per molar of sugar in solution.

In the upper right panel, $k_{\text{on}}[c]$ is plotted versus $[c]$ and appears linear. The nonzero $[c] = 0$ intercept may result from channel gating: nanotubes exhibit voltage-dependent contractions even in the absence of sugar [17]. Allowing for a nonzero intercept, a linear fit gives $k_{\text{on}} = 4.0\ \text{s}^{-1}\ \mu\text{M}^{-1}$. This is much smaller than the diffusion-limited capture rate per molar $k_{\text{app}} = 4DaN_A$ where a is the nanotube diameter, D is the diffusion coefficient of sugar and N_A is Avogadro's number [30,31]. Using $a \approx 0.5$ nm, we have $k_{\text{app}} \approx 200k_{\text{on}}$, so only $1/200$ of the molecules that diffuse to the mouth of the monomer become stably bound within it.

Turning to detrapping, $B(t)$ drops rapidly for $t < 0.01$ s by an amount that depends on $[c]$. For $t > 0.01$ s, it is described by

$$B(t) \approx -a - k_{\text{off}}t \quad (\text{for } t > 0.01\ \text{s}), \tag{3}$$

where the empirical parameters a and k_{off} are independent of t. From Fig. 3, k_{off} is independent of $[c]$ with a value of roughly $50\ \text{s}^{-1}$. The extrapolated intercept a decreases with $[c]$.

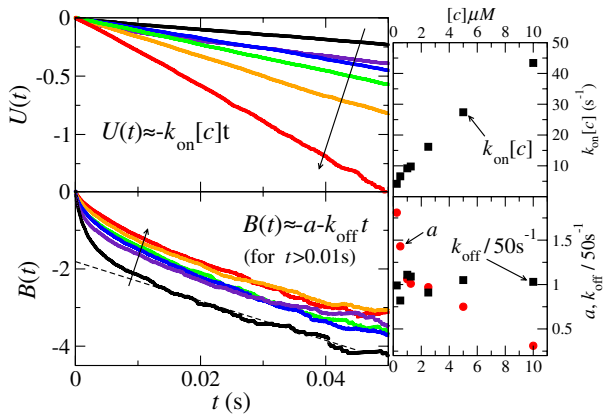

FIG. 3 (color online). Evidence for multiple-molecule trapping by a monomer. Left panels: Horizontal axis is time t and vertical axis is logarithm of the probability that a monomer remains unblocked (upper panel) or blocked (lower panel) for longer than t, denoted by $U(t)$ or $B(t)$. Curves are for different sugar concentrations $[c]$, along arrows: $[c] = 0.25$, 0.5, 1.0, 2.5, 5, and 10 μM. For $t > 0.01$, linear fits to $B(t)$ (the dashed line) can be made, but the low-t nonlinear behavior indicates multiple trapping states. Upper right: slope $k_{\text{on}}[c]$ of linear fit to $U(t)$, versus $[c]$. Lower right: Slope k_{off} and extrapolated $t = 0$ intercept a, from linear fit to $B(t)$ for $t > 0.01$ s, versus $[c]$.

Consider the t and $[c]$ dependence of $B(t)$. At small t, the steep slope describes fast detrapping. Fast detrapping plays an important role at low $[c]$, causing a large drop of $B(t)$, but has less effect at high $[c]$. On a longer t scale, the slow detrapping rate $k_{\text{off}} \approx 50\ \text{s}^{-1}$ sets in. Slow detrapping is most important at high $[c]$ (the fraction of occupied monomers that empty via the slow process is $\exp(-a)$, which increases with $[c]$). The natural interpretation of this behavior is that there are at least two binding states, with different detrapping rates, that can be simultaneously occupied. Fast detrapping affects singly occupied monomers, and slow detrapping affects multiply occupied monomers. As $[c]$ increases, multiple occupation becomes more likely and slow detrapping dominates.

A simple model provides more detail [25]. We use a model monomer with two traps, 1 and 2, that act in series, with 1 nearer the cis end. The monomer can be blocked in three ways (a molecule in trap $\alpha = 1$, 2 or in both, which we denote by $\alpha = 3$). At $t = 0$, the monomer has a probability $p_\alpha(t = 0) = \delta^1_\alpha$ to be in state α. Then $d\mathbf{p}/dt = \mathbf{M} \cdot \mathbf{p}$, where $\mathbf{M}$ is a matrix and $\mathbf{p}$ a vector with components p_α, determines the probability at later t. We have

$$B(t) = \ln\Big(\sum_j \Lambda_j \exp[\mu_j t]\Big), \tag{4}$$

where μ_j are eigenvalues of $\mathbf{M}$, rows of $\mathbf{m}$ are eigenvectors of $\mathbf{M}$, and $\Lambda_j = \Sigma_{\alpha,\beta} p_\alpha(0) m^{-1}_{\alpha,j} m_{j,\beta}$.

A molecule detraps from $\alpha = 1$, 2 at a rate k_α and hops from 1 to 2 at a rate x_+ (or x_- in reverse). These processes are included in a matrix $\mathbf{M}_0$. A smaller term $\mathbf{M}_1$ couples to $\alpha = 3$ with $\mathbf{M} = \mathbf{M}_0 + \mathbf{M}_1$. $\mathbf{M}_1$ includes $\tilde{k}_{\text{on}}[c]$, the trapping rate of a monomer with a molecule in trap 2, and $\tilde{k}_\alpha$, the rate at which a doubly occupied monomer empties trap α. Both molecules detrap at once at a rate $\tilde{k}_{12}$ with $\tilde{k} = \tilde{k}_1 + \tilde{k}_2 + \tilde{k}_{12}$.

To first order in $\mathbf{M}_1$ and at large t, Eq. (4) gives Eq. (3) with

$$k_{\text{off}} = \tilde{k}, \qquad a = -\ln\Big(\frac{\tilde{k}_{\text{on}}[c]x_+}{k_1k_2 + k_2x_+ + k_1x_-}\Big). \tag{5}$$

The large-t slope is constant and equal to the total detrapping rate of a doubly occupied monomer. In Fig. 4, calculations of $B(t)$ are shown. All curves use the same parameters, except for $\tilde{k}_{\text{on}}[c]$, which increases along the arrow: $\tilde{k}_{\text{on}}[c] = 3$, 6, 9, 12, and $15k_1$, respectively. We used: $k_1 = x_- = (1/2)k_2 = (1/20)x_+ = 40\ \text{s}^{-1}$, also $\tilde{k}_1 = \tilde{k}_2 = 0$ and $\tilde{k}_{12} = 51\ \text{s}^{-1}$. There are too many parameters to take quantitative fits seriously but the model captures all aspects of the qualitative behavior of $B(t)$.

We can use transition state theory [32] to estimate the molecular current q. Figure 4 shows the free energy for a monomer with single (ST) and double traps (DT). The

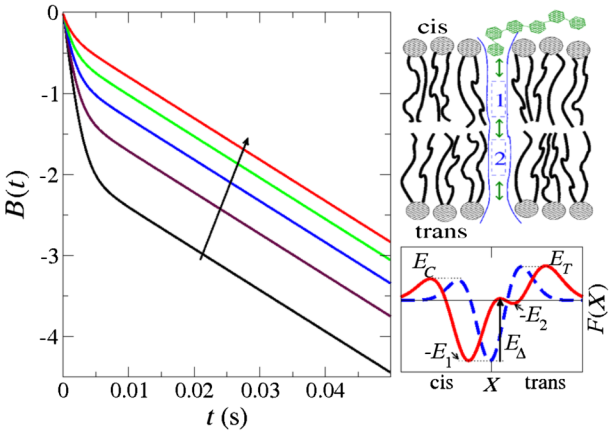

FIG. 4 (color online). Model calculation of $B(t)$ based on a monomer with two traps. Left panel: Calculated $B(t)$ with parameters given in text. The only parameter that varies across curves is the trapping rate of an occupied monomer, which increases along arrow to model increasing concentration. Upper right: Schematic of two-trap model. Lower right: Effective free energy F versus reaction coordinate X for models with one (dashed) or two (solid) traps. The energy barriers, E_C on outside (cis), E_T on inside (trans) and trap level $-E_1$ are common to both models. The two-trap model has another level at $-E_2$, protected by barrier E_Δ.

barriers on the cis and trans ends are E_C and E_T. There is a trap level at $-E_1$ for ST, with frequency ω_1, and levels at $-E_1$ and $-E_2$ for DT, with frequencies ω_1 and ω_2. Molecules hopping from 1 to 2 see a barrier E_Δ. The molecular currents (net rate of molecules passing from cis to trans) are q_{ST} and q_{DT} for ST and DT. Assuming sugar cannot escape the cell interior and ignoring interactions between molecules, we obtain $q_{\mathrm{ST}} = k_{\mathrm{on}}[c]/(1+a)$ and $q_{\mathrm{DT}} = k_{\mathrm{on}}[c]/(1+Za)$ where $a = \mathrm{e}^{\beta[E_T-E_C]} + (k_{\mathrm{on}}[c]/\omega_1)\mathrm{e}^{\beta[E_1+E_T]}$, with $\beta = 1/(k_BT)$ and $Z = (1+\eta)/(1+\theta q_{\mathrm{DT}}/[\eta\omega_1])$ with $\ln\eta = \beta(E_\Delta - E_1 - E_T)$ and $\theta = 1-(\omega_1/\omega_2)\mathrm{e}^{\beta[E_2-E_1]}$. At low $[c]$ ST is more effective, but at high $[c]$, DT can be advantageous [33].

Since *V. harveyi* degrades chitin locally, ChiP may see bursts of high-$[c]$ diffusion current during which a multiple-trap design is preferable. A greater benefit of multiple traps could be realized if molecules in the monomer attractively interact (which was not included in the q_{DT} calculation). From the fit of the model to $B(t)$, the $[c]$ dependence was explained if the first molecule enhances the trapping rate of a second and if both molecules detrap together, which implies attraction. (Note that the longer dwell time of a molecule in a doubly occupied monomer was not simply explained by one molecule blocking the escape of another.) An empty monomer captures a small fraction of incident molecules, but if one bound molecule helps draw others, then the bacterium can well utilize a brief window to uptake sugar in rough water.

In conclusion, we studied ChiP, the nanotubes used by marine bacteria to uptake sugar. By interpreting ion current fluctuations in terms of the trapping or detrapping of sugar molecules, we found that ChiP utilizes multiple traps within a nanotube and exploits correlations between trapped molecules—a novel strategy that enables bacteria to achieve high sugar translocation rates in extreme environments.

M. F. S. was supported by Suranaree University of Technology and the Higher Education Research Promotion and National Research University Project of Thailand, Office of the Higher Education Commission. W. S. was supported by the Thailand Research Fund (Grant No. RMU5380055) and Alexander von Humboldt Foundation, Germany. $I(t)$ measurements were done in the lab of M. Winterhalter at Jacobs University Bremen.

*mfsmith@g.sut.ac.th

[1] T. Schirmer, T. A. Keller, Y. F. Wang, and J. P. Rosenbusch, Science **267**, 512 (1995).
[2] M. Winterhalter, Curr. Opin. Colloid Interface Sci. **5**, 250 (2000).
[3] E. Berkane, F. Orlik, A. Charbit, C. Danelon, D. Fournier, R. Benz, and M. Winterhalter, J. Nanobiotechnol. **3**, 3 (2005).
[4] L. Kullman, P. A. Gurnev, M. Winterhalter, and S. M. Bezrukov, Phys. Rev. Lett. **96**, 038101 (2006).
[5] B. Austin and X.-H. Zhang, Lett. Appl. Microbiol. **43**, 119 (2006).
[6] C. E. Zobell and S. C. Rittenberg, J. Bacteriol. **35**, 275 (1938).
[7] N. O. Keyhani, X. B. Li, and S. Roseman, J. Biol. Chem. **275**, 33 068 (2000).
[8] N. O. Keyhani and S. Roseman, Biochim. Biophys. Acta, Gen. Subj. **1473**, 108 (1999).
[9] X. Li and S. Roseman, Proc. Natl. Acad. Sci. U.S.A. **101**, 627 (2004).
[10] B. L. Bassler, C. Yu, C. Y. C. Lee, and S. Roseman, J. Biol. Chem. **266**, 24 276 (1991).
[11] D. E. Hunt, D. Gevers, N. M. Vahora, and M. F. Polz, Appl. Environ. Microbiol. **74**, 44 (2007).
[12] C. Pruzzo, L. Vezzulli, and R. R. Colwell, Environ. Microbiol. **10**, 1400 (2008).
[13] K. K. Meibom, X. B. Li, A. T. Nielsen, C. Y. Wu, S. Roseman, and G. K. Schoolnik, Proc. Natl. Acad. Sci. U.S.A. **101**, 2524 (2004).
[14] W. Suginta, W. Chumjan, K. R. Mahendran, P. Janning, A. Schulte, and M. Winterhalter, PLoS ONE **8**, e55126 (2013).
[15] R. Dutzler, Y.-F. Wang, P. J. Rizkallah, J. P. Rosenbusch, and T. Schirmer, Structure **4**, 127 (1996).
[16] Y.-F. Wang, R. Dutzler, P. J. RIzkallah, J. P. Rosenbusch, and T. Schirmer, J. Mol. Biol. **272**, 56 (1997).
[17] C. Hilty and M. Winterhalter, Phys. Rev. Lett. **86**, 5624 (2001).
[18] S. M. Bezrukov, L. Kullman, and M. Winterhalter, FEBS Lett. **476**, 224 (2000).
[19] W. Suginta, W. Chumjan, K. R. Mahendran, A. Schulte, and M. Winterhalter, J. Biol. Chem. **288**, 11038 (2013).

[20] C. Andersen, M. Jordy, and R. Benz, J. Gen. Physiol. **105**, 385 (1995).
[21] C. Andersen, R. Cseh, K. Schüelein, and R. Benz, J. Membr. Biol. **164**, 263 (1998).
[22] E. G. Saravolac, N. F. Taylor, R. Benz, and R. R. Hancock, J. Bacteriol. **173**, 4970 (1991).
[23] F. Orlik, C. Andersen, C. Danelon, M. Winterhalter, M. Pajatsch, A. Bock, and R. Benz, Biophys. J. **85**, 876 (2003).
[24] G. Scwharz, C. Danelon, and M. Winterhalter, Biophys. J. **84**, 2990 (2003).
[25] See Supplemental Material at http://link.aps.org/supplemental/10.1103/PhysRevLett.110.238102 for additional information about experimental and analytical procedure.
[26] M. Montal and P. Mueller, Proc. Natl. Acad. Sci. U.S.A. **69**, 3561 (1972).
[27] C. Danelon, T. Brando, and M. Winterhalter, J. Biol. Chem. **278**, 35 542 (2003).
[28] C. Anderson, B. Schiffler, A. Charbitt, and R. Benz, J. Biol. Chem. **277**, 41318 (2002).
[29] J. J. Kasianowicz, J. Robertson, E. Chan, J. Reiner, and V. M. Stanford, Annu. Rev. Anal. Chem. **1**, 737 (2008).
[30] H. C. Berg and E. M. Purcell, Biophys. J. **20**, 193 (1977).
[31] P. C. Bressloff and J. M. Newby, Rev. Mod. Phys. **85**, 135 (2013).
[32] P. Hanggi, P. Talkner, and M. Borkovec, Rev. Mod. Phys. **62**, 251 (1990).
[33] At low $[c]$, $q_{\mathrm{DT}}/q_{\mathrm{ST}} \approx (1+a)/(1+aZ) < 1$. At large $[c]$ q_{ST} saturates at $q_{\mathrm{ST}}^{\max} = \omega_1 e^{\beta[-E_1 - E_T]}$ and q_{DT} at $q_{\mathrm{DT}}^{\max} = \omega_1 e^{\beta[-E_1 - E_T]}(1+\eta-\theta e^{-\beta E_\Delta})^{-1}$, so $q_{\mathrm{DT}}^{\max} > q_{\mathrm{ST}}^{\max}$ if $e^{-\beta E_\Delta}\theta > \eta$.